J. Fluid Mech. (1988), *vol.* 186, *pp.* 25–46
Printed in Great Britain

Time-dependent response of floating ice to a steadily moving load

By R. M. S. M. SCHULKES and A. D. SNEYD
University of Waikato, Hamilton, New Zealand

(Received 18 November 1986 and in revised form 11 June 1987)

When a steadily moving load is applied to a floating ice plate, the disturbance will generally approach a steady state (relative to the load) as time $t \to \infty$. However, for certain 'critical' load speeds the disturbance may grow continuously with time, which represents some danger to vehicles driving on ice. To understand this phenomenon and the overall time development of the ice response, this paper analyses the problem of an impulsively applied, concentrated line load on a perfectly elastic homogeneous floating ice plate. An exact expression for the ice deflection is derived, and then interpreted by means of asymptotic expansions for large t in the vicinity of the source. The spatial development of the disturbance is analysed by considering asymptotic expansions as $t \to \infty$ near an observer moving away from the load. Theoretical results are compared with field measurements, and some hitherto unexplained features can be understood.

1. Introduction

Floating ice is often used as a roadway or aircraft runway, and to estimate operational safety one needs a theory describing the response of a floating ice plate to a moving load. Such a theory can also be used to estimate ice parameters such as Young's modulus E or viscoelastic constants, from measurements of the response to a known load. The first theoretical study appears to have been a paper by Greenhill (1887) who derived a dispersion relation for waves in a perfectly elastic, homogeneous ice plate, floating above water of uniform depth. Wilson (1958) observed that if the vehicle speed V were less than the minimum phase speed $c_{\min}$ for free waves, the ice response would be similar to the deflection due to a static load, whereas if V were greater than $c_{\min}$, waves would be generated. He also showed how to calculate the wavelengths, and pointed out that the greatest response can be expected when the vehicle speed V is equal to $c_{\min}$. Kheisin (1963) studied in detail the effect of a steadily moving point and line load, and found general expressions for the ice displacement. He concluded that for the line load there were two 'critical speeds' near which the steady deflection was unbounded, whereas for the point load there were no such critical speeds. Nevel (1970) extended Kheisin's analysis to deal with a uniform load distributed over a circular area, and found that Kheisin's second conclusion was incorrect – that there indeed exists a critical speed, and that such singularities are not just artefacts of two-dimensionality. Kerr (1983) identified mathematically this critical speed as the minimum phase speed $c_{\min}$. Obviously, deflections cannot become infinite as V approaches the critical speed, and Nevel suggested nonlinear effects, dissipation or inhomogeneity of the ice, as possible explanations. However Kheisin (1971) realized that the most likely explanation was time dependence – since Nevel's (and his own earlier) analysis assumed a steady deflection, the load had

effectively remained in contact with the ice for an infinite time. Kheisin then analysed the effect of an impulsively applied steadily moving line load and found that when $V = c_{\min}$ the ice deflection grows continuously in time as $t^{\frac{1}{3}}$. Unfortunately this paper is rather inaccessible and seems to contain several errors of detail in the asymptotic analysis. A simple physical explanation of this growth rate was given by Davys, Hosking & Sneyd (1985), who observed that this critical speed also coincided with the group speed of the waves. Bates & Shapiro (1981) have discussed the effect of viscoeleasticity on the ice response, and shown that this will eventually limit the growth of the deflection when $V = c_{\min}$. Kerr (1981) has given a comprehensive survey of the literature concerning loads moving across elastic plates supported by fluid or Winkler (spring) bases.

Recent experimental studies of ice waves by Eyre (1977), Beltaos (1980), Takizawa (1985) and Squire *et al.* (1985) have largely agreed with theoretical predictions. It is now known just how the ice response varies with speed, and that maximum deflections occur when $V = c_{\min}$ – indeed the load speed at which maximum deflections occur can be used as an estimate of $c_{\min}$ and hence of E (Squire *et al.* 1985). It is legendary that to drive a vehicle across ice can be dangerous at certain speeds, and Eyre (1977) mentions that 'apocryphal tales from northern Canada suggest that vehicles can create enormous ice waves under certain circumstances'. Recently Takizawa (1985) and Squire *et al.* (1985) have independently measured amplification of the ice response due to a vehicle moving at speed $c_{\min}$, but find it much less than the viscoelastic limit derived by Bates & Shapiro (1981).

The aim of the present paper is to study the effect of an impulsively applied concentrated line load moving with uniform speed, as originally proposed by Kheisin (1971), and to investigate a number of time-dependent effects which are important in interpreting field measurements. In §2 we derive an expression for the Fourier transform of ice displacement, and in §3 we use the method of steepest descent to find asymptotic expansions of the displacement as $t \to \infty$, in the vicinity of the source. Like Kheisin (1971) we find that the ice response is static for $V < c_{\min}$, wavelike for $V > c_{\min}$ and grows as $t^{\frac{1}{3}}$ when $V = c_{\min}$, but our formulae differ in amplitude and phase. We also find a second 'critical speed' $V = (gH)^{\frac{1}{2}}$, where H is water depth and g acceleration due to gravity, at which the ice displacement grows as $t^{\frac{1}{3}}$. In §4 we investigate the spatial development of the wave system by considering asymptotic limits of the displacement as seen by an observer moving away from the source, and find, as expected, that wavelike disturbances are propagated away from the source with the relative group speeds, while at the two critical speeds $V = c_{\min}$ and $V = (gH)^{\frac{1}{2}}$ the propagation speeds decrease with time as $t^{-\frac{1}{4}}$ and $t^{-\frac{2}{3}}$ respectively. We also present results showing the time development of the disturbance, which have been calculated using a fast Fourier inversion of the formula derived in §2, and show that the main features can be understood in terms of the simple asymptotic formulae given in §§3 and 4. Finally, §5 compares our results with the various field measurements, and resolves a number of anomalies.

2. Expression for surface displacement

Consider an infinite homogeneous ice sheet of thickness h and density ρ_i floating on water of density ρ as shown in figure 1. The upper undisturbed water surface is $z = 0$ and the sea bed $z = -H$. If $\eta(x, y, t)$ represents a small vertical ice-sheet deflection then the equation of motion of the ice sheet is

$$D\nabla^4\eta + \rho_i h\eta_{tt} = -\rho(\phi_t)_{z=0} - \rho g\eta - f(x, y, t) \tag{2.1}$$

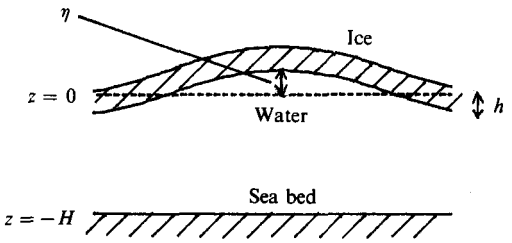

FIGURE 1. Diagram of ice–water system.

(see e.g. Davys *et al.* 1985). Here

$$D = \frac{Eh^3}{12(1-\nu^2)}$$

is the modulus of rigidity of the ice sheet (E being Young's modulus and ν Poisson's ratio for ice), $f(x, y, t)$ the downward external stress (or load) exerted on the ice, and ϕ the velocity potential for the flow under the ice. In future we neglect the ice acceleration term – the second term on the left-hand side of (2.1) – which is justified provided the wavelength of the surface displacement is much larger than the ice thickness h. Since the water motion penetrates to a depth comparable with one wavelength, the inertia of the thin ice plate will then be small compared with that of the moving-water layer. Unless otherwise stated, we shall use following typical parameter values for McMurdo Sound in Antarctica (cf. Davys *et al.* 1985): $E = 5\times10^9\ \mathrm{Nm^{-2}}$, $h = 2.5$ m, $H = 350$ m, $\nu = \frac{1}{3}$, and $\rho = 10^3\ \mathrm{kg/m^3}$.

2.1. *Single-Fourier-component load*

Consider a one-dimensional (y-independent) load applied at $t = 0$ and thereafter moving with constant velocity $V\hat{\boldsymbol{x}}$, so that the loading function is of the form

$$f(x, y, t) = g(x - Vt)H(t), \tag{2.2}$$

where H is the Heaviside step function. We begin by analysing the effect of a single Fourier component of g – i.e. a loading function of the form $\mathrm{e}^{\mathrm{i}k(x-Vt)}$ – and anticipate that η and ϕ will exhibit a similar x-dependence:

$$\eta = \hat{\eta}(k, t)\,\mathrm{e}^{\mathrm{i}kx}, \quad \phi = \hat{\phi}(k, z, t)\,\mathrm{e}^{\mathrm{i}kx}.$$

Because ϕ satisfies Laplace's equation, and the kinematic conditions

$$(\phi_z)_{z=-H} = 0, \quad (\phi_z)_{z=0} = \eta_t,$$

one can show that

$$(\phi)_{z=0} = \frac{1}{k}\coth(kH)\,\eta_t. \tag{2.3}$$

Substituting (2.3) into (2.1) then gives

$$Dk^4\hat{\eta} + \frac{\rho}{k}\coth(kH)\,\hat{\eta}_{tt} + \rho g\hat{\eta} = -\mathrm{e}^{-\mathrm{i}kVt}. \tag{2.4}$$

The general solution of (2.4) is

$$\hat{\eta}(k, t) = A\,\mathrm{e}^{\mathrm{i}kct} + B\,\mathrm{e}^{-\mathrm{i}kct} - \frac{\mathrm{e}^{-\mathrm{i}kVt}}{Dk^4 + \rho g - \rho kV^2\coth(kH)}, \tag{2.5}$$

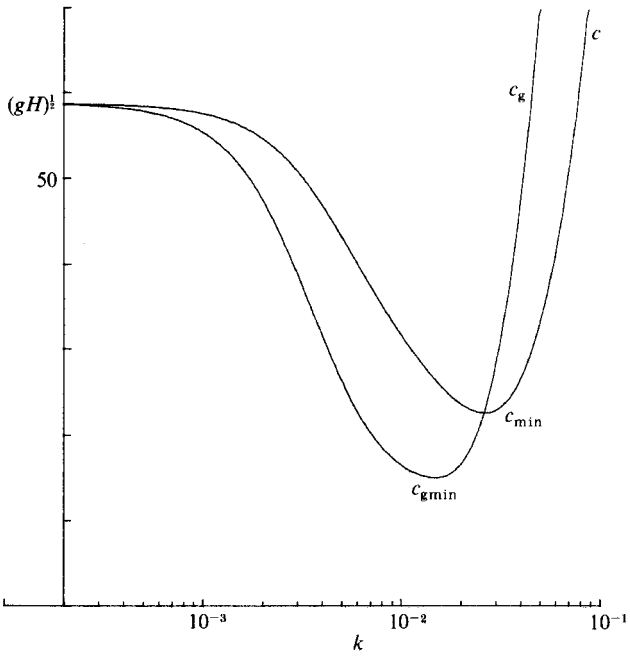

FIGURE 2. Graphs of phase velocity c and group velocity c_g in m/s against wavenumber k in m^{-1}. Note that the wavenumber scale is logarithmic.

where A and B are arbitrary constants and

$$c^2 = \left(\frac{Dk^4}{\rho} + g\right)\frac{1}{k}\tanh(kH). \tag{2.6}$$

The first two terms on the right-hand side of (2.5) represent free waves travelling with speed $c(k)$ given by the dispersion relation (2.6), and the last represents the forced wave. The constants A and B are found from the initial conditions

$$(\eta)_{t=0} = 0, \quad (\eta_t)_{t=0} = 0,$$

and we obtain,

$$\hat{\eta}(k,t) = \frac{e^{-ikVt}(e^{-i\psi_1 t}-1)}{2\rho c(k)\psi_1(k)}\tanh(kH) + \frac{e^{-ikVt}(e^{i\psi_2 t}-1)}{2\rho c(k)\psi_2(k)}\tanh(kH). \tag{2.7}$$

Here ψ_1, ψ_2 are phase functions defined by

$$\psi_1(k) = k(c-V), \quad \psi_2(k) = k(c+V). \tag{2.8}$$

The solution for the general loading function (2.2) is found by superposing Fourier components:

$$\eta(x,t) = \frac{1}{(2\pi)^{\frac{1}{2}}}\int_{-\infty}^{\infty} \hat{g}(k)\,\hat{\eta}(k,t)\,e^{ikx}\,dk,$$

where $\hat{\eta}$ is given by (2.7), and $\hat{g}$ is the Fourier transform of g, defined by

$$\hat{g}(k) = \frac{1}{(2\pi)^{\frac{1}{2}}}\int_{-\infty}^{\infty} e^{-ikx}g(x)\,dx.$$

In particular for a concentrated line load $g(x-Vt) = F\delta(x-Vt)$, where δ is the Dirac delta function and F a constant representing the applied force per unit length in the y-direction, we have $\hat{g} = 1/(2\pi)^{\frac{1}{2}}$, and

$$\eta(x,t) = \frac{F}{2\pi}\int_{-\infty}^{\infty} \hat{\eta}(k,t)\, \mathrm{e}^{\mathrm{i}kx}\, \mathrm{d}k \tag{2.9}$$

is the formal solution. Note that $\hat{\eta}(k,t)$ is an analytic function of k in some neighbourhood of the real axis, since $c^2(k)$ is positive for real k, and zeros of ψ_1 will be cancelled by corresponding zeros in the numerator. A formula equivalent to (2.7) and (2.9) has been given by Kheisin (1971).

Figure 2 shows graphs of the free wave speed $c(k)$ and group speed $c_g(\mathrm{k}) = \mathrm{d}(ck)/\mathrm{d}k$ against k for the McMurdo Sound parameters. Note that both c and c_g attain minimum values, $c_{\min} = 22.5$ m/s and $c_{\mathrm{gmin}} = 14.9$ m/s.

3. Asymptotic expansion for large time in the vicinity of the source

We introduce a coordinate $X = x - Vt$ moving with the source. Now (2.7) and (2.9) can be combined and written in the form

$$\eta = \frac{F}{2\pi\rho}(I_1 + I_2 - I_0), \tag{3.1}$$

where $I_0 = \int_{-\infty}^{\infty} \frac{\mathrm{e}^{\mathrm{i}kX}}{\psi_1(k)\,\psi_2(k)} k \tanh(kH)\,\mathrm{d}k$, $I_1 = \int_{-\infty}^{\infty} \frac{\mathrm{e}^{\mathrm{i}(kX-\psi_1 t)}}{2c(k)\,\psi_1(k)} \tanh(kH)\,\mathrm{d}k$, (3.2*a*, *b*)

and $$I_2 = \int_{-\infty}^{\infty} \frac{\mathrm{e}^{\mathrm{i}(kX+\psi_2 t)}}{2c(k)\,\psi_2(k)} \tanh(kH)\,\mathrm{d}k. \tag{3.2c}$$

For convenience we shall also denote the integrand in each integral I_i by $N_i(k)$, $i = 0, 1, 2$. Note that the integral I_0 is time-independent.

We expand the integrals asymptotically using the method of steepest descents. This involves deforming the contour of integration from the real line in the complex k-plane by a displacement $-\mathrm{i}\delta/\psi'(k)$ (δ being some small positive quantity), so that on the deformed contour the absolute value of $\mathrm{e}^{-\mathrm{i}\psi(k)t}$ is $\mathrm{e}^{-\delta t}$ – exponentially small as $t \to \infty$. This contour deformation fails at points where $\psi'(k) = 0$ – i.e. at points of stationary phase – and the disjoint branches of the deformed contour must be linked by a straight-line path of steepest descent (cf. Lighthill 1978, figure 63). Such links contribute the terms that dominate the integral for large time, and which are generally $O(t^{-\frac{1}{2}})$, unless ψ'' also vanishes at the point of stationary phase, in which case they are $O(t^{-\frac{1}{3}})$.

Since $\psi_2(k)$ is monotonically increasing its derivative is always strictly positive and no points of stationary phase occur, so we conclude that the integral I_2 vanishes exponentially as $t \to \infty$. We consider only those terms which decay algebraically with time, and accordingly I_2 is neglected.

The phase function $\psi_1(k)$ is an odd function of k and its behaviour depends crucially on the source speed V, figure 3 illustrating the various possibilities. Since ψ_1 has real zeros for $V \geqslant c_{\min}$ the integrands $N_0(k)$, $N_1(k)$ may have real poles: but since the combined integrand $\hat{\eta}(k,t)\,\mathrm{e}^{\mathrm{i}kx}$ is analytic in some neighbourhood of the real axis, contour deformation is permissible. Points of stationary phase (i.e. zeros of $\psi_1'(k)$) will be denoted by $k = k_A, k_B$, zeros of $\psi_1(k)$ by $k = k_Y, k_Z$, and points where both ψ_1 and ψ_1' vanish by $k = k_M$.

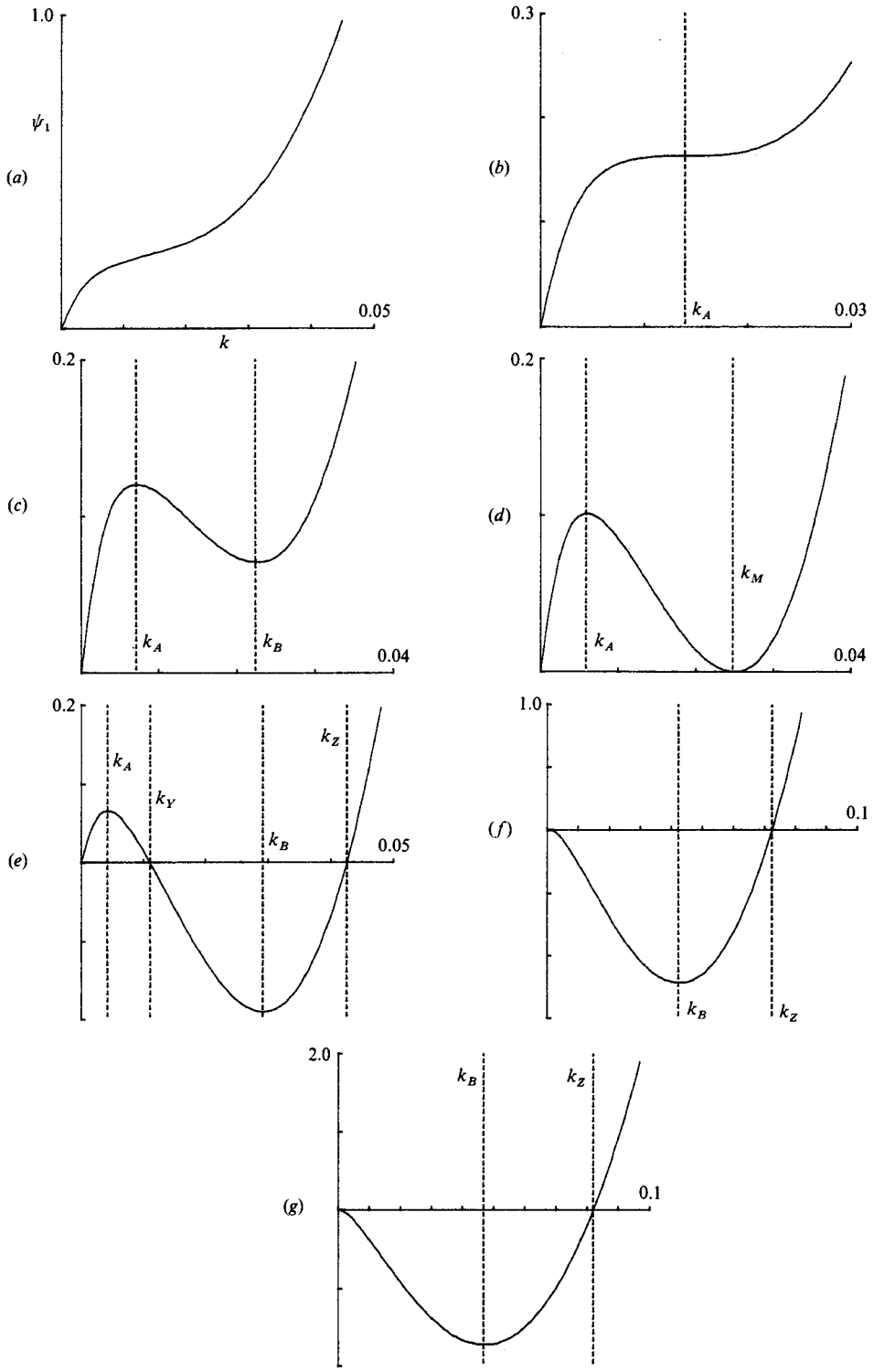

FIGURE 3. Graphs of the phase function $\psi_1 = k(c-V)$ in s^{-1} against wavenumber k in m^{-1}, for various representative source speeds: (*a*) $V = 10 < c_{gmin}$; (*b*) $V = 14.9 = c_{gmin}$; (*c*) $c_{gmin} < V = 20 < c_{min}$; (*d*) $V = 22.5 = c_{min}$; (*e*) $c_{min} < V = 30 < (gH)^{\frac{1}{2}}$; (*f*) $V = (gH)^{\frac{1}{2}} = 58.6$; (*g*) $V = 70 > (gH)^{\frac{1}{2}}$.

3.1. *Source speeds V for which the disturbance approaches a steady state*

Case (i): Subcritical speeds, $V < c_{\min}$

For subcritical speeds ψ_1 has no real zeros, and the integrands $N_0(k)$, $N_1(k)$, are analytic in some neighbourhood of the real axis. The integral $I_1 \to 0$ as $t \to \infty$ by the Riemann–Lebesgue lemma, so the ultimate steady surface displacement is given by

$$\eta_s(X, V) = \frac{-F}{2\pi\rho} I_0. \tag{3.3}$$

When $V = 0$, I_0 can be expressed analytically to give

$$\eta_s(X, 0) = \frac{-Fl^3}{4\sqrt{2}D} \exp\left(-\frac{|X|}{l}\right) \cos\left(\tfrac{1}{4}\pi - \frac{|X|}{l}\right), \tag{3.4}$$

where $l = (4D/\rho g)^{\frac{1}{4}} \approx 42$ m is a characteristic lengthscale. Equation (3.4) represents the static deflection due to a line load F placed on the ice. Figure 4 shows graphs of the steady deflection $\eta_s(X, V)$ against X for various V, which are symmetric about the origin since I_0 is an even function of X. These have been obtained numerically using a fast Fourier inversion of (3.3). Since $V < c_{\min}$ wavecrests can never remain stationary with respect to the source – they will always overtake it – so the steady ice deflection is not wavelike but similar in form to the static deflection (3.4). As V approaches $c_{\min}$ however, η_s becomes larger and more oscillatory.

To discuss the leading time-dependent terms in I_1 we further subdivide the source speed range.

Case (i)a: $V < c_{\text{gmin}}$

In this case ψ_1 is a monotonically increasing function of k (figure 3*a*), so there are no points of stationary phase. It follows that I_1 decays exponentially with time, and the steady state is approached relatively rapidly.

Case (i)b: $V = c_{\text{gmin}}$

Now ψ_1 has a point of inflexion at $k = k_A$ say (figure 3*b*), and I_1 is of order $t^{-\frac{1}{3}}$ for large time. Specifically we can write

$$\eta = \eta_s + \eta_0 \alpha_A \left(\frac{t_A}{t}\right)^{\frac{1}{3}} \cos(k_A X - \psi_{1A} t),$$

where the maximum static deflection per unit force, $-\eta_s(0, 0) = Fl^3/8D = \eta_0$, provides a displacement scale, and the modulation timescale t_A and modulation coefficient α_A are given by

$$t_A = \frac{6}{k_A^3 |c''_{gA}|}, \quad \alpha_A = \frac{4\Gamma(\frac{1}{3}) D \tanh(k_A H)}{\sqrt{3}\pi\rho l^3 c_A (c_A - V)}.$$

We use the subscript A to denote the value of a variable at $k = k_A$ and the prime to denote differentiation with respect to k. For the McMurdo Sound parameters we find the timescale t_A is 15.6 s, and the coefficient $\alpha_A = 0.220$, so the transients die away quite slowly.

Case (i)c: $c_{\text{gmin}} < v < c_{\min}$

There are two points k_A, k_B of stationary phase (see figure 3*c*) and we can write

$$\eta = \eta_s + \eta_0 \alpha_A \left(\frac{t_A}{t}\right)^{\frac{1}{2}} \cos(k_A X - \psi_{1A} t + \tfrac{1}{4}\pi) + \eta_0 \alpha_B \left(\frac{t_B}{t}\right)^{\frac{1}{2}} \cos(k_B X - \psi_{1B} t - \tfrac{1}{4}\pi),$$

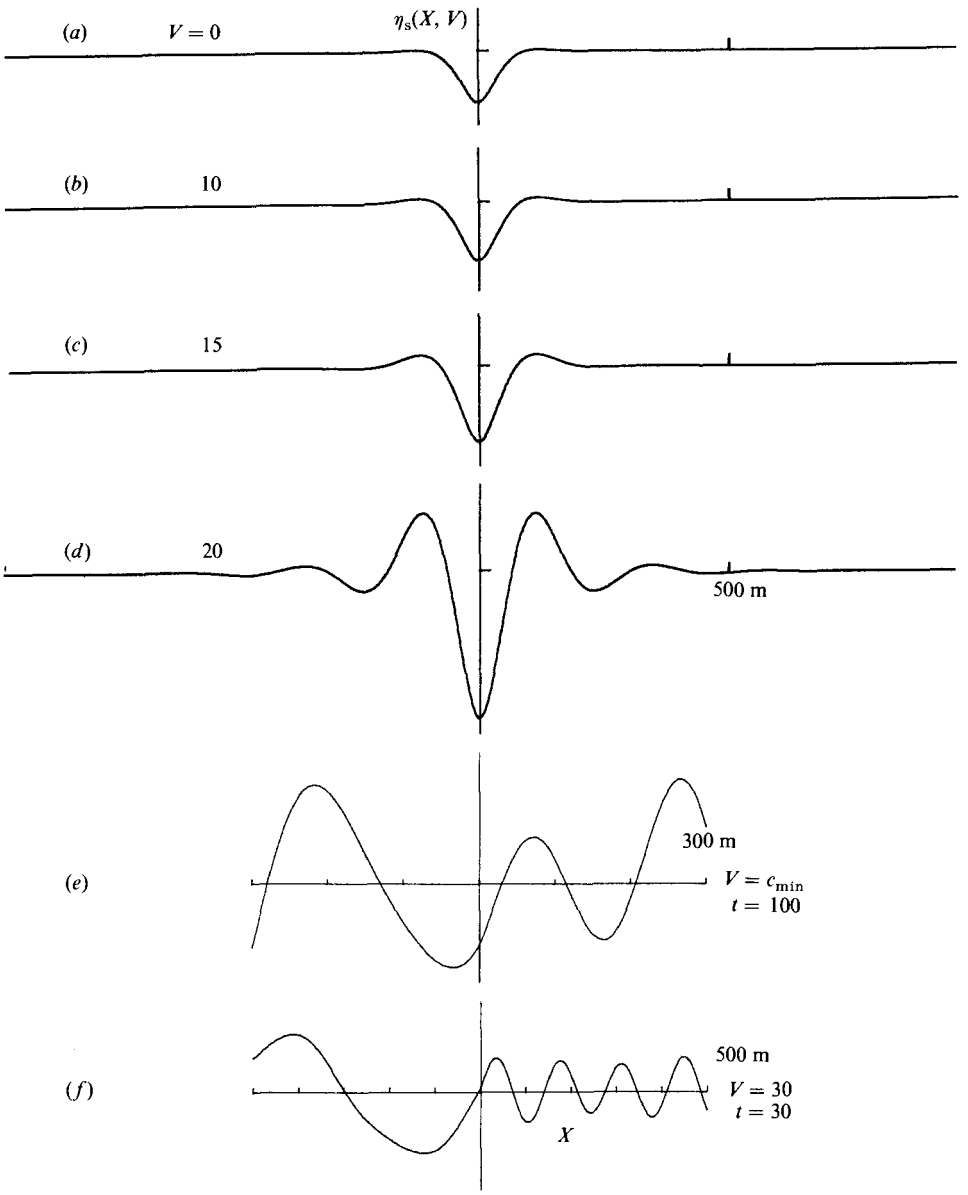

FIGURE 4. (*a–d*) The steady ice displacement for various subcritical source speeds. (*e*) The displacement when $V = c_{\min}$ and $t = 100\ s$, according to the asymptotic formula (3.10). (*f*) The displacement when $c_{\min} < V = 30$ m/s $< (gH)^{\frac{1}{2}}$, and $t = 30$ s, according to the asymptotic formula (3.7). The ultimate steady waveform is slightly modulated by transients.

where the modulation times t_A, t_B and modulation coefficients α_A, α_B are given by

$$t_A = \frac{2\pi}{k_A^2 |c'_{gA}|}, \quad \alpha_A = \frac{\tanh(k_A H)}{4\pi\rho c_A (c_A - V)\eta_0} \text{etc.}$$

For $V = 18$ m/s the McMurdo Sound parameters give $t_A = 72.3$ s, $\alpha_A = 0.115$, $t_B = 15.7$ s, and $\alpha_B = 0.571$.

Case (ii): Super-critical speeds, $c_{\min} < V < (gH)^{\frac{1}{2}}$

When the source speed becomes supercritical the phase function ψ_1 has two positive and two negative zeros on the real k-axis: $k = \pm k_Y$, $k = \pm k_Z$ say (figure 3*e*). Since the integrand $\hat{\eta}(k,t)\,\mathrm{e}^{\mathrm{i}kx}$ is analytic in some neighbourhood of the real axis, we may deform the contour of integration to one on which $|\mathrm{e}^{-\mathrm{i}\psi_1 t}| = \mathrm{e}^{-\delta t}$, together with four steepest-descent links across the points of stationary phase at $k = \pm k_A$, $k = \pm k_B$. The positive half of this contour is shown in figure 5 (*a*). Now ψ_1 will have no zeros on the deformed contour C, so we write

$$\eta = \frac{-F}{2\pi\rho} I_{0C} + \frac{F}{2\pi\rho} I_{1C},$$

where the integrals I_{0C}, I_{1C}, are as defined in (3.2*a*, *b*) except that the path of integration is C instead of the real axis. As before the first term represents the ultimate steady state, and the second the transient response.

The steady term can be evaluated by contour integration. For $X > 0$ the contour C is closed by a large semicircle $|k| = R$ in the *upper* half-plane, along which the integral tends to zero as $R \to \infty$ by Jordan's lemma. Thus the residue theorem gives

$$\eta_{\mathrm{s}}(X) = \frac{-\mathrm{i}F}{\rho} \Sigma \text{ residues above } C \text{ of } N_0(k).$$

Two of the poles in question occur at $k = \pm k_Z$ (where $c(k_Z) = V$) and the sum of these residues gives a contribution to η_{s} of

$$\frac{F \sin(k_Z X)}{\rho V(c_{gZ} - V)} \tanh(k_Z H).$$

The function $N_0(k)$ also has an infinite sequence of poles on the imaginary axis. Using (2.5) we can write

$$N_0(\mathrm{i}s) = \frac{\mathrm{i}\rho \mathrm{e}^{-sX}}{Ds^4 + \rho g - \rho V^2 s \cot(sH)}, \quad (s \text{ real}).$$

It is easily seen that the denominator will have an infinite sequence of zeros $\{s_n\}$, $n = 1, 2, \ldots$ where $n\pi/H < s_n < (n+1)\pi/H$. The residues at these poles can be written in the form $-\mathrm{i}\gamma_n \mathrm{e}^{-s_n X}$ where $\gamma_n = O(n^{-7})$ as $n \to \infty$ (see Schulkes 1986). Thus contributions from these poles to η_{s} will be important only in the vicinity of the source, and for the first few n. To summarize, we can write

$$\eta_{\mathrm{s}} = \frac{F \sin(k_Z X)}{\rho V(c_{gZ} - V)} \tanh(k_Z H) + R(X) \quad (X > 0), \tag{3.5}$$

where

$$R(X) = \frac{F}{\rho} \sum_{n=1}^{\infty} \gamma_n \mathrm{e}^{-s_n X},$$

and the constants γ_n, s_n may be calculated numerically.

For negative X the contour C must be completed in the *lower* half-plane, and

$$\eta_{\mathrm{s}} = \frac{\mathrm{i}F}{\rho} \Sigma \text{ residues below } C \text{ of } N_0(k).$$

This time the real poles occur at $k = \pm k_Y$ and as before we find

$$\eta_{\mathrm{s}} = \frac{F \sin(k_Y X)}{\rho V(V - c_{gY})} \tanh(k_Y H) + R(-X) \quad (X < 0). \tag{3.6}$$

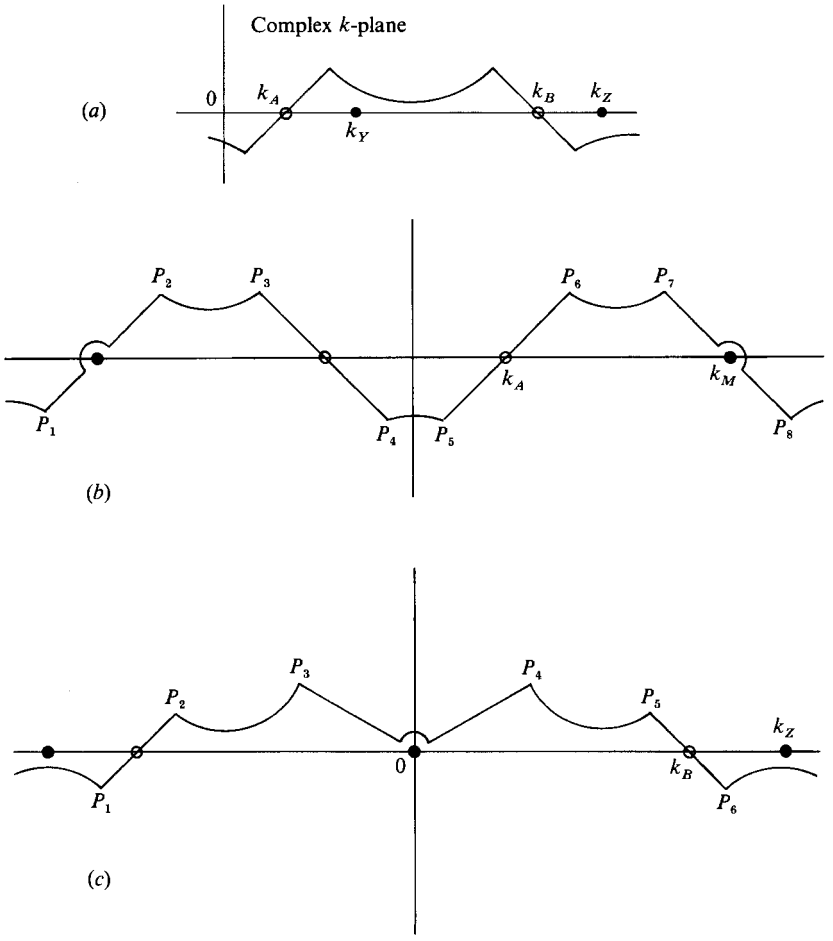

FIGURE 5. Integration contours (*a*) for $c_{\min} < V < (gH)^{\frac{1}{2}}$; (*b*) for $V = c_{\min}$ and (*c*) for $V = (gH)^{\frac{1}{2}}$: The open circles denote points of stationary phase, and the solid circles, zeros of ψ_1.

The displacement consists essentially of the two plane waves whose phase speeds are equal to the source speed, so that the crests appear stationary relative to the source. The short wavelength ($k = k_Z$) appears ahead of the source because its group speed is greater than the source speed ($c_{gZ} > V$), and conversely the long wavelength ($k = k_Y$) appears behind.

The time-dependent integral I_{1C} has four points of stationary phase $k = \pm k_A$, $k = \pm k_B$, which give the dominant contributions, of order $t^{-\frac{1}{2}}$, as $t \to \infty$. One can write

$$\eta = \frac{F \tanh(k_Z H)}{\rho V(c_{gZ} - V)} \left[\sin(k_Z X) + \alpha_A \left(\frac{t_A}{t}\right)^{\frac{1}{2}} \cos(k_A X - \psi_{1A} t + \tfrac{1}{4}\pi) \right.$$
$$\left. + \alpha_B \left(\frac{t_B}{t}\right)^{\frac{1}{2}} \cos(k_B X - \psi_{1B} t + \tfrac{3}{4}\pi) \right] + R(X) \quad (X > 0), \quad (3.7)$$

where the modulation times t_A, t_B and modulation coefficients α_A, α_B are given by

$$t_A = \frac{2\pi}{k_A^2 |c'_{gA}|}, \quad \alpha_A = \frac{V(c_{gZ} - V) \tanh(k_A H)}{4\pi c_A (c_A - V) \tanh(k_Z H)}, \text{ etc.}$$

The equation for η when $X < 0$ is similar, except that the subscript Y replaces Z, and the sign of the coefficient of $\sin(k_Y X)$ is reversed. For a source speed of 30 m/s the timescales t_A, t_B are 61.6 s and 3.83 s respectively. Figure 4(*f*) shows the ice displacement at time $t = 30$ s for $V = 30$ m/s calculated using (3.7) and the corresponding equation for negative X. Modulation by the transients is still evident, and since the term $R(|X|)$ was ignored there is a slight discontinuity at the origin.

Case (iii) : $V > (gH)^{\frac{1}{2}}$

At higher source speeds ($V > (gH)^{\frac{1}{2}}$) there is only one point of stationary phase ($k = k_B$) and only one zero ($k = k_Z$) of ψ_1. The expressions for η can be obtained from (3.5), (3.6) and (3.7) simply by setting $k_Y = \alpha_A = 0$.

3.2. *Source speeds V for which the displacement does not tend to a steady state*

Case (iv) : $V = c_{\min}$

When $V = c_{\min}$ the zeros k_Y, k_Z of ψ_1 and the zero k_B of ψ_1' coincide at $k = k_M$ say, where ψ_1 will have a double zero (figure 3*d*). The contour C must therefore be indented around k_M to avoid the double pole of N_0 (see figure 5*b*). The integral I_{0C} can be evaluated by the residue theorem as before :

$$\frac{-F}{2\pi\rho} I_{0C} = \begin{cases} R(X), & (X > 0); \\ \dfrac{-F}{\rho V}[X w_M \cos(k_M X) + w_M' \sin(k_M X)] + R(-X), & (X < 0), \end{cases} \tag{3.8 a, b}$$

where

$$w(k) = \frac{\tanh(kH)(k-k_M)^2}{\psi_1(k)}.$$

The integrand $N_1(k)$ will be exponentially small on C apart from the straight-line segments P_3P_4, P_5P_6 and the indented segments P_1P_2, P_7P_8. The former give the usual stationary phase contributions of $O(t^{-\frac{1}{2}})$, while the latter give rise to integrals of the form considered in the Appendix which will be dominant for large time – a term $O(t^{\frac{1}{2}})$ and a time-independent term similar to the first in (3.8*b*).

To find the contribution from P_7P_8 we use the substitution $z = \mathrm{i}(k - k_M)$ to rotate the contour into the form considered in the Appendix. This gives

$$\int_{P_7P_8} N_1(k)\,\mathrm{d}k = \mathrm{i}\int_{C_\epsilon} \frac{w(k_M - \mathrm{i}z)\,\mathrm{e}^{\mathrm{i}k_M X + Xz}}{2c(k_M - \mathrm{i}z)} \frac{\mathrm{e}^{\mathrm{i}z^2\tau}}{z^2}\,\mathrm{d}z + O(\mathrm{e}^{-at}),$$

where a is a positive constant and $\tau = \frac{1}{2}\psi_1''(k_M)\,t$. From (A 8) then,

$$\int_{P_7P_8} N_1(k)\,\mathrm{d}k = \frac{\mathrm{e}^{\mathrm{i}k_M X}}{V}[-w_M\,\mathrm{e}^{\mathrm{i}\pi/4}(\pi\tau)^{\frac{1}{2}} + \pi X w_M - \pi\mathrm{i}w_M'].$$

The contribution from P_1P_2 can be evaluated directly from (A 8), and when the two are combined we find

$$\int_{P_1P_2+P_7P_8} N_1(k)\,\mathrm{d}k = \frac{-w_M}{V}\cos(k_M X + \tfrac{1}{4}\pi)\,(\pi\tau)^{\frac{1}{2}} + \frac{\pi X w_M}{V}\cos(k_M X) + \frac{\pi w_M'}{V}\sin(k_M X). \tag{3.9}$$

Finally, combining (3.8) and (3.9) :

$$\eta = \frac{F w_M}{\rho V k_M}\left[-\left(\frac{t}{t_M}\right)^{\frac{1}{2}}\cos(k_M X + \tfrac{1}{4}\pi) + |k_M X|\cos(k_M X) + \alpha\sin(k_M|X|)\right] + R(|X|) + O(t^{-\frac{1}{2}}), \tag{3.10}$$

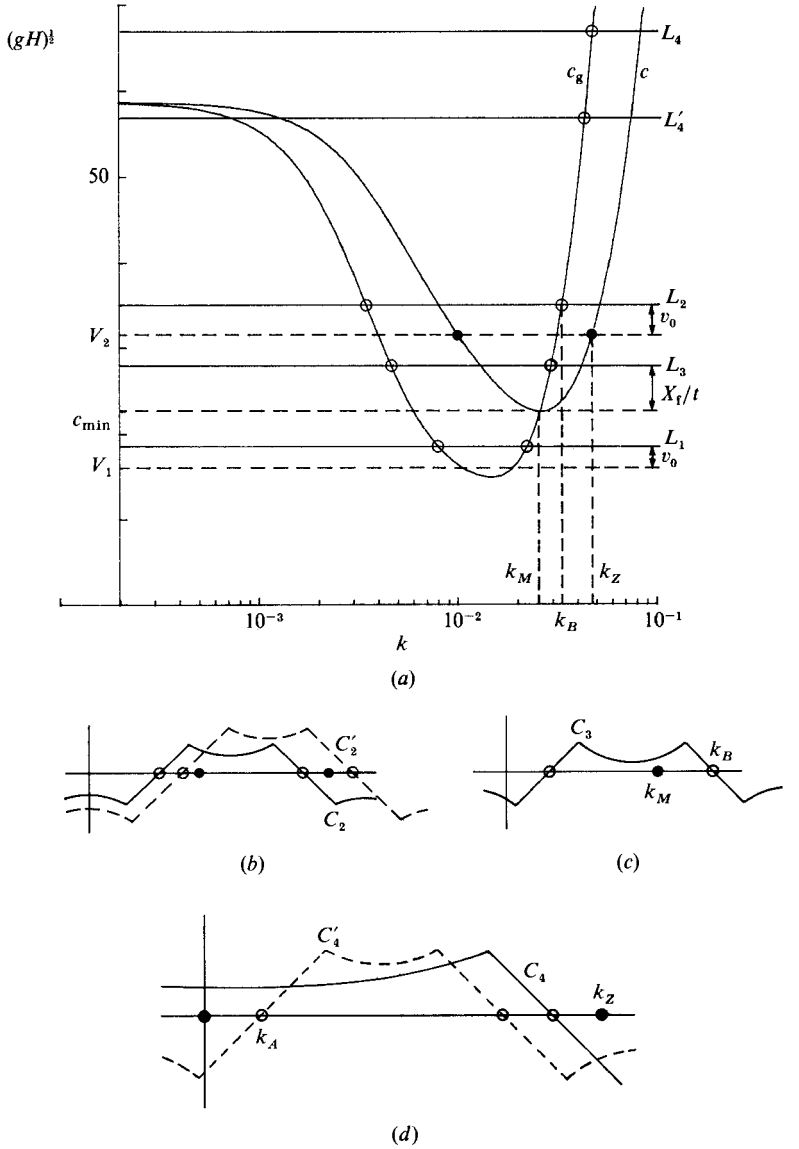

FIGURE 6. (*a*) The construction of stationary-phase points for the displacement viewed by an observer moving away from the source. (*b–d*) Integration contours used when $c_{\min} < V < (gH)^{\frac{1}{2}}$, $V = c_{\min}$ and $V = (gH)^{\frac{1}{2}}$ respectively. The open circles indicate points of stationary phase, and the solid circles, zeros of ψ_1.

where $\alpha = k_M w_M'/w_M$ and the growth timescale $t_M = 2\pi/k_M^2 c_{gM}'$. A graph of ice displacement in the vicinity of the source, calculated from (3.10), is shown in figure 4(*e*).

The most striking feature of (3.10) is that the displacement grows in time as $t^{\frac{1}{2}}$ (cf. Kheisin 1971). The physical explanation given by Davys *et al.* (1985) is that at this particular source speed, $V = c = c_g$ so the wave-energy propagation speed equals the source speed. Thus energy accumulates continuously in the vicinity of the source where the energy density will grow linearly with time. Since energy density is proportional to η^2, it follows that η will grow as $t^{\frac{1}{2}}$.

Case (v) : $V = (gH)^{\frac{1}{2}}$

At this speed the points $\pm k_A$, $\pm k_Y$ all merge together at the origin, where the odd function $\psi_1(k)$ will have a triple zero. The contour C must be indented about this point, as shown in figure 5(*c*).

The integral I_{0C} is evaluated by the residue theorem :

$$\frac{-F}{2\pi\rho} I_{0C} = \begin{cases} \dfrac{F \tanh(k_Z H)}{\rho V(c_{gZ} - V)} \sin(k_Z X) + R(X), & (X > 0), \\ \dfrac{3FX}{\rho H V^2} + R(-X), & (X < 0). \end{cases} \tag{3.11a, b}$$

The integrand $N_1(k)$ is exponentially small on C except along the straight segments P_1P_2, P_5P_6 which give contributions $O(t^{-\frac{1}{2}})$, and the indented segment P_3P_4 which gives the dominant term $O(t^{\frac{1}{3}})$. This latter term is of the form considered in the Appendix ($n = 3$), and (A 9) gives

$$\int_{P_3P_4} N_1(k)\,\mathrm{d}k = \frac{3\Gamma(\frac{2}{3})\sqrt{3}}{V^2}\left(\frac{t}{t_0}\right)^{\frac{1}{3}} - \frac{2\pi X}{HV^2}, \quad t_0 = 6\left(\frac{H}{g}\right)^{\frac{1}{2}}. \tag{3.12}$$

Combining (3.11) and (3.12) we find

$$\eta = \begin{cases} \dfrac{F \tanh(k_Z H)}{\rho V(c_{gZ} - V)} \sin(k_Z X) + \dfrac{F}{\rho V^2}\left[\beta\left(\dfrac{t}{t_0}\right)^{\frac{1}{3}} - \dfrac{X}{H}\right] + R(X) & (X > 0); \\ \dfrac{F}{\rho V^2}\left[\beta\left(\dfrac{t}{t_0}\right)^{\frac{1}{3}} + \dfrac{2X}{H}\right] + R(-X), & (X < 0), \end{cases} \tag{3.13a, b}$$

where $\beta = 3\sqrt{3}\Gamma(\frac{2}{3})/2\pi$. The displacement again grows unboundedly as $t \to \infty$ because $V = c = c_g$, but now the wavelength for which this triple equality occurs is a *limiting wavelength* ($\lambda = 2\pi/k \to \infty$) so the singularity is weaker. One might anticipate this singularity, since in (3.6) $|\eta_s| \to \infty$ as $V \to (gH)^{\frac{1}{2}}$ and $c_{gY} \to V$.

4. Spatial development of the wave system

In §3 we considered the asymptotic limit $t \to \infty$ with X fixed, which yields a description of the ice displacement in the neighbourhood of the origin. Clearly formulae such as (3.10) can be valid only when X is not too large, and indeed the Riemann–Lebesgue lemma implies that the ice displacement must tend to zero as $X \to \pm\infty$ *for fixed* t. When interpreting experimental records it is important to have a picture of the way in which the disturbance spreads out from the source with time, and to this end we consider a different kind of asymptotic limit – the limit as $t \to \infty$ of the displacement seen by an observer moving away from the source with constant relative speed v_0. In other words we write $X = v_0 t + X_0$ so that X_0 is a coordinate relative to the observer, and take the asymptotic limit $t \to \infty$ *with* X_0 *fixed*.

In the integrand N_1 we rewrite

$$\mathrm{e}^{\mathrm{i}(kX - \psi_1 t)} \quad \text{as } \mathrm{e}^{\mathrm{i}(kX_0 - \bar{\psi}_1 t)}, \quad \bar{\psi}_1 = k[c - (V + v_0)].$$

Points of stationary phase are now determined by

$$\frac{\mathrm{d}\bar{\psi}_1}{\mathrm{d}k} = 0 \quad \text{or } c_g(k) = V + v_0. \tag{4.1}$$

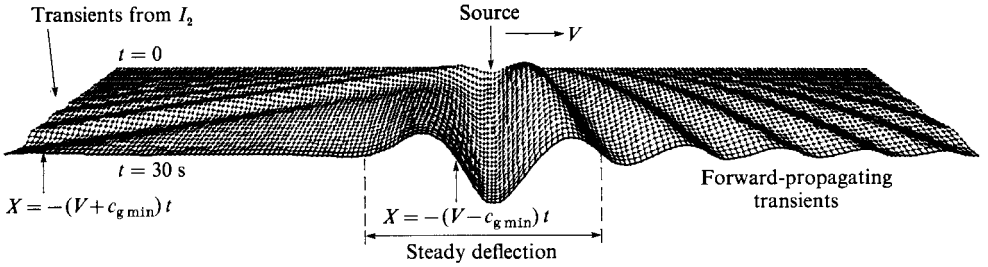

FIGURE 7. Time development of the ice displacement for $V = 18$ m/s $< c_{min}$.

4.1. *Source speeds V for which the disturbance tends to a steady state*

Case (i) : Sub-critical speeds, $V < c_{min}$

For fixed $X_0, X \to \pm\infty$ as $t \to \infty$ and the integral $I_0 \to 0$ by the Riemann–Lebesgue lemma. The integral I_1 can be written in the form

$$I_1 = \int_{-\infty}^{\infty} \frac{e^{i(kX_0 - \bar{\psi}_1 t)}}{2c(k)\,\psi_1(k)} \tanh(kH)\,dk,$$

and will contribute stationary-phase terms of $O(t^{-\frac{1}{2}})$ as $t \to \infty$. Thus no matter how slowly the observer moves away from the source, he will eventually enter a region in which η is very small ; in other words the disturbance does not propagate away from the source, which is consistent with the idea (cf. §3) that it is static rather than wavelike.

To examine the propagation of the transients let us consider a source moving with speed V_1, where $c_{gmin} < V_1 < c_{min}$. The transients in the vicinity of the moving observer will arise from the points of stationary phase determined by (4.1), and shown in figure 6(*a*) as the points of intersection of the line L_1 with the group-velocity curve. If the observer is moving ahead of the source ($v_0 > 0$) there will be at least two points of stationary phase, so the observer will always be in the presence of transients decaying as $t^{-\frac{1}{2}}$. On the other hand, if $v_0 < c_{gmin} - V_1 < 0$ the corresponding line does not intersect the group velocity curve – i.e. there will be no points of stationary phase and the disturbance in the vicinity of the observer decays exponentially. This means that the $t^{-\frac{1}{2}}$ transients cannot penetrate the region $X < -(V_1 - c_{gmin})\,t$, where the displacement will rapidly tend to zero. Figure 7 shows time development of the wave system for $V = 18$ m/s, computed directly from (2.9) by means of a fast-Fourier-transform routine. The transients ahead of the source are evident, as is the quiescent region behind the marked point $X = -(V_1 - c_{gmin})\,t$.

Case (ii) : Super-critical speeds, $c_{min} < V < (gH)^{\frac{1}{2}}$

Consider a source moving with speed V_2 in this range, and an observer moving ahead with positive relative velocity v_0. When v_0 is small the point k_B of stationary phase, determined by the intersection of the line L_2 with the c_g curve in figure 6(*a*), is to the left of the pole k_Z, and the corresponding integration contour C_2 is shown in figure 6(*b*). The steady displacement for $X > 0$ is found by evaluating I_0 using the residue theorem applied to the closed contour formed by C_2 and a large semicircle in the upper half-plane. This contour includes the pole k_Z so the observer sees the steady forward wave. As v_0 increases however, the point of stationary phase k_B moves to the right and eventually passes to the right of k_Z. The completion of the corresponding integration contour C_2' (figure 6*b*) now excludes the pole k_Z, and

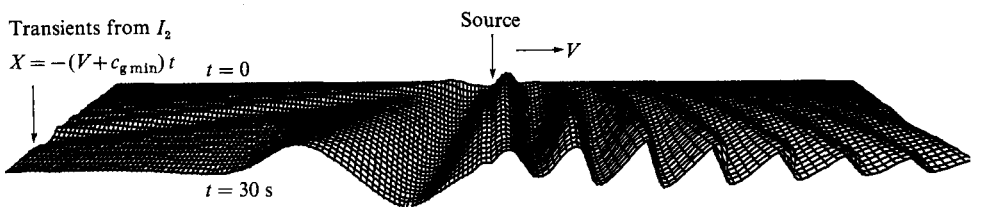

FIGURE 8. Time development of the wave system for $c_{\min} < V = 30$ m/s $< (gH)^{\frac{1}{2}}$.

the observer sees only decaying transients. The transition ($k_B = k_Z$) occurs when $v_0 = c_{gZ} - V_2$.

These arguments show just what one would expect – that the forward steady wave propagates outward from the source with the relative group speed $c_{gZ} - V_2$. Similarly one can show that the trailing wave propagates behind the source with relative speed $V_2 - c_{gY}$. Figure 8 shows the time development of the wave system for $V = 30$ m/s, again computed from (2.9) by a fast Fourier transform. The group speed of the leading wave relative to the source ($c_{gZ} - V$) is 30.5 m/s and the wavelength is 138 m, so over a period of 30 s about 7 wavelengths have been generated. In contrast, the relative group speed of the trailing wave ($V - c_{gY}$) is 14.2 m/s and the wavelength 571 m, so only one wavelength has been generated over the same period.

Case (iii) : Super-critical speeds, $V > (gH)^{\frac{1}{2}}$

This is very similar to case (ii) – waves are propagated forwards away from the source with the relative group speed $c_{gZ} - V$.

4.2. *Source speeds V for which the displacement does not tend to a steady form*

Case (iv) : $V = c_{\min}$

If an observer moves ahead of the source with constant speed $v_0 > 0$ the integration contour will be similar to C_2' in figure 6(*b*), so no steady deflection will be observed. The disturbance does not therefore propagate forward at any finite constant speed, as one would expect since the group speed is equal to the source speed.

To investigate the disturbance propagation in more detail we consider an observer moving with the 'disturbance front' whose position at time t is given by

$$X = X_f(t).$$

We expect $X_f(t)$ to be a function that increases with t at a rate somewhat less than linear. As before we introduce X_0 as a coordinate relative to the observer, so that $X = X_f(t) + X_0$ and

$$e^{i(kX - \psi_1 t)} = e^{i(kX_0 - \bar{\psi}_1 t)}, \quad \bar{\psi}_1 = k[c - (V + t^{-1}X_f(t))],$$

so the points of stationary phase occur where

$$c_g(k) = V + \frac{X_f(t)}{t}, \tag{4.2}$$

(i.e. at the points where the line L_3 (figure 6*a*) intersects the group-velocity curve). Since we expect $X_f(t)/t$ to be small for large t, the greater of the two solutions of (4.2),

$k = k_B$, will be close to k_M where $c = c_{\min} = c_g = V$. Expanding $c_g(k)$ as a Taylor series about k_M in (4.2) gives

$$c'_{gM}(k_B - k_M) = t^{-1}X_f(t) \quad \text{so } k_B - k_M = \frac{X_f(t)}{tc'_{gM}}. \tag{4.3}$$

Thus as t increases the point k_B of stationary phase approaches k_M from the right. Since the integration contour C_3 for $X_0 > 0$ (figure 6*c*) excludes the pole at k_M, the steady contribution from the integral I_0 vanishes, but the stationary phase contribution from I_1 yields

$$\eta = \frac{F\tanh(k_B H)}{4\pi\rho V\psi_{1B}}\left(\frac{2\pi}{tc'_{gB}}\right)^{\frac{1}{2}}\cos(\bar{\psi}_{1B}t - k_B X_0 + \tfrac{1}{4}\pi). \tag{4.4}$$

Since ψ_1 has a double zero at k_M, the Taylor series expansion near this point will be $\psi_1 = \frac{1}{2}c'_{gM}(k-k_M)^2$, and using (4.3) and (4.4) we find that the amplitude of η is

$$\frac{F\tanh(k_B H)}{(2\pi)^{\frac{1}{2}}\rho V^2}\frac{Vc'_{gM}t^{\frac{3}{2}}}{(c'_{gB})^{\frac{1}{2}}X_f^2}.$$

Since the observer is situated at the ' leading edge ' of the disturbance, the amplitude of the local deflection remains constant as $t \to \infty$ and $k_B \to k_M$, which implies that

$$X_f(t) = t^{\frac{3}{4}}V^{\frac{1}{2}}(c'_{gM})^{\frac{1}{4}} = 28.5t^{\frac{3}{4}}\text{ m}$$

for the McMurdo Sound parameters.

Similar analysis shows that the trailing edge of the disturbance is given by $X = -X_f(t)$. Thus the disturbance spreads in both directions at a speed decreasing as $t^{-\frac{1}{4}}$ for large time.

Case (v) : $V = (gH)^{\frac{1}{2}}$

Again we write $X = X_f(t) + X_0$, where $X_f(t)$ is the position of an observer moving with the disturbance front. For a forward-moving observer, $X_f > 0$ and there is just one point of stationary phase where the line L_4 (figure 6*a*) intersects the group-velocity curve. The corresponding integration contour C_4 is shown in figure 6(*d*) and the situation is similar to case (ii) – an elastic wave of wavenumber k_Z propagating forward at the relative group speed $c_{gZ} - V$, modulated by $t^{-\frac{1}{2}}$ transients.

For a backward-moving observer the situation is quite different. Now the line L'_4 (figure 6*a*) determines a stationary-phase point k_A close to the origin, and the corresponding integration contour C'_4 is shown in figure 6(*d*). For small k the dispersion relation (2.6) assumes the approximate form

$$c = V(1 - \tfrac{1}{6}k^2H^2), \quad \text{with } c_g = V(1 - \tfrac{1}{2}k^2H^2). \tag{4.5}$$

From the stationary-phase condition (4.2) it follows that

$$k_A^2 = \frac{2X_f(t)}{VH^2t}, \tag{4.6}$$

where now for simplicity we have taken X_f to be positive so that the position of the disturbance front is $X = -X_f$. The amplitude of the stationary-phase contribution from $k = k_A$ is

$$\frac{F\tanh(k_A H)}{4\pi\rho V\psi_{1A}}\left(\frac{2\pi}{|c'_{gA}|\,t}\right)^{\frac{1}{2}}, \tag{4.7}$$

and from (4.5), $$\psi_{1A} = -\tfrac{1}{6}Vk_A^3H^2, \quad c'_{gA} = -Vk_AH^2. \tag{4.8}$$

Combining (4.6), (4.7) and (4.8) we find that the stationary-phase amplitude is

$$\frac{-3F}{2^{\frac{7}{4}}\pi^{\frac{1}{2}}\rho V^2}\left(\frac{V^3H^2t^3}{X_f^5}\right)^{\frac{1}{4}}.$$

Since the amplitude in the vicinity of this observer will be constant, we obtain

$$X_f(t) = H^{\frac{2}{5}}V^{\frac{3}{5}}t^{\frac{3}{5}} = 119t^{\frac{3}{5}}\text{ m}$$

for the McMurdo Sound parameters. Thus the disturbance which grows as $t^{\frac{1}{5}}$ (see (3.13)) propagates *only behind* the source, at a speed that decreases as $t^{-\frac{2}{5}}$ for large time.

So far we have ignored the integral I_2 in (3.1) for the reasons outlined in §3. If we again consider an observer moving with constant speed v_0 and write $X = X_0 + v_0 t$, then in the numerator of $N_2(k)$ we rewrite

$$e^{i(kX+\psi_2 t)} \quad \text{as} \quad e^{i(kX_0+\bar{\psi}_2 t)}, \quad \bar{\psi}_2 = k(c+V+v_0).$$

This integral will therefore give rise to a stationary-phase transient seen by an observer moving rear-ward with a speed greater than or equal to $V + c_{\text{gmin}}$. Such transients can be seen in figures 7 and 8, where points $X = -(V+c_{\text{gmin}})t$ are marked.

5. Comparison with experiment

Recent field observations confirm that the form of the ice deflection changes with source speed, according to the theory of §3. Eyre (1977) and Takizawa (1985) distinguish the following five source-speed regimes:

(*a*) A low-speed regime, $V < 0.6$–$0.7c_{\text{min}}$ when the deflection has the same shape as the static deflection, as illustrated in figure 4(*a*, *b*).

(*b*) An early transition regime 0.6–$0.7c_{\text{min}} < V < 0.85c_{\text{min}}$ during which the depression becomes deeper and narrower, and the rim rises progressively, as shown in figure 4(*c*).

(*c*) A late transition regime when $V \approx c_{\text{min}}$ where a wavelike pattern begins to appear both behind and in front of the source, and the depression centre lags behind the source, as illustrated in figure 4(*d*, *e*).

(*d*) A two-wave regime $c_{\text{min}} < V < (gH)^{\frac{1}{2}}$ with a short elastic wave in front and long gravity wave behind, when the ice displacement is given by (3.5) and (3.6).

(*e*) A single-wave regime $V > (gH)^{\frac{1}{2}}$ with waves propagating only ahead of the source.

It seems likely that the transition from regimes (*a*) to (*b*) occurs when V is close to c_{gmin} – the speed at which wavelike transients first appear. The ratio $c_{\text{gmin}}/c_{\text{min}}$ is 0.72 for the physical parameters in Eyre's (1977) experiments, and 0.80 for Takizawa's (1985). No observations of the growing displacement propagated behind the source when $V = (gH)^{\frac{1}{2}}$ (equation (3.15)) have been reported, perhaps because the unlimited growth at this second critical speed has not previously been analysed. Another possible reason is that this growing displacement is uniform – i.e. of infinite wavelength – and would not register on instruments that measure the slope (Beltaos 1980) or curvature (Squire *et al.* 1985) of the ice surface. It is also possible that $V = (gH)^{\frac{1}{2}}$ does not represent a critical speed for *two-dimensional sources*, because wave energy could radiate in all directions – not just along the line of motion. On the other hand we would expect $V = c_{\text{min}}$ to be a critical speed even for two-dimensional sources, since at this speed the wavecrests are all parallel and perpendicular to the

line of motion, so energy can be propagated only along this line (see Davys *et al.* 1985, discussion on p. 278). An analysis of the two-dimensional time-dependent problem is needed to resolve this question.

Squire *et al.* (1985) and Takizawa (1985) give results for the 'amplification factor' – the ratio of the maximum displacement or stress at $V = c_{\min}$ to that at $V = 0$. Both authors invoke dissipation (e.g. ice viscoelasticity) to explain why this factor is finite, rather than infinite as predicted by the steady-state analysis of Nevel (1970). From (3.10) it is clear however that even without dissipation the displacement at $V = c_{\min}$ will be limited by *the time that the source has been travelling*. Indeed (3.4) shows that the maximum static deflection is

$$\frac{Fl^3}{8D}, \quad l = \left(\frac{4D}{\rho g}\right)^{\frac{1}{4}}.$$

so from (3.10) we find the amplification factor,

$$f_{\mathrm{A}} = \frac{16D \tanh(k_M H)}{l^3 \rho V k_M c'_{gM}} \left(\frac{t}{t_M}\right)^{\frac{1}{2}}.$$

In the Takizawa (1985) experiments the vehicle travelled about 100 m at constant speed before reaching the observation point – a travel time of $100/c_{\min} = 16.6$ s. This figure gives $f_{\mathrm{A}} = 6.6$, compared with the observed value of about 3.0. The discrepancy may be due to viscoelastic damping, or perhaps experimental difficulties in locating the resonance peak. Squire *et al.* (1986) plot a graph of strain against vehicle speed (their figure 5.3) which shows a very sharp peak at $V = c_{\min}$, indicating that very accurate control of vehicle speed would be necessary to measure the true maximum value. Squire *et al.* (1985) measured the amplification of the *ice stress*, or equivalently the ice curvature. When $V = 0$ (3.4) shows that the curvature at the point of maximum depression is $Fl/4D$, so the stress amplification factor f_{S} can be found using (3.10):

$$f_{\mathrm{S}} = \frac{8Dk_M \tanh(k_M H)}{l\rho V c'_{gM}} \left(\frac{t}{t_M}\right)^{\frac{1}{2}}. \tag{5.1}$$

The length of the vehicle track was 500 m, so assuming instantaneous acceleration we put $t = 500/c_{\min} = 32$ s in (5.1), and obtain $f_{\mathrm{S}} = 5.0$, which again is about twice the observed values, which range from 2.24 to 2.29. Bates & Shapiro (1981) estimate that viscoelasticity would impose a limit of about 5.0 on the maximum observable value of f_{S}, so from (5.1) we see that experimental track lengths should be quadrupled to ensure that f_{S} is indeed limited by viscoelasticity and not by vehicle run-up time.

Both Squire *et al.* (1985) and Takizawa (1985) have measured the wavelengths of the steady waves established in the two-wave regime (*d*). While both authors find good agreement with theory for the leading elastic-dominated waves, the trailing gravity waves appear somewhat shorter than theory would predict (see figures 6 and 5 in the respective papers). Our explanation again relates to the establishment time. In §4 we showed that waves propagate outwards from the source with the relative group speed $c_{\mathrm{g}} - V$, so the number of complete wavelengths λ generated in time t is $t|c_{\mathrm{g}} - V|/\lambda$. Table 1 lists, for various source speeds, the number of wavelengths that would have been generated when the observations by the above authors were made. In each case several complete leading elastic waves have been propagated, but where the trailing-gravity-wave observations disagree with theory, less than one complete wavelength has been generated.

Eyre (1977), Takizawa (1985) and Beltaos (1980) all note that the point of

Author	Squire *et al.* (1985)			Takizawa (1985)		
V	17.0	20.0	22.0	6.5	7.5	8.0
n_E	3.6	7.0	9.0	3.4	7.6	9.3
n_g	1.1	0.93	0.79	0.86	0.26	0.03
$\lambda_{obs}/\lambda_{theo}$	1	0.9	0.77	1	0.58	0.34

TABLE 1. The number n_E of leading elastic waves, and n_g of trailing gravity waves propagated at the time of observation. The last row of the table shows the ratio of the observed gravity wavelength to its theoretical value. In all cases the elastic wavelengths show good agreement with theory.

maximum depression begins to lag behind the source as V approaches c_{min}. This effect can be seen in figure 4(*e*), and (3.10) specifies that the point of maximum depression should occur one-eighth of a wavelength behind the source. Takizawa (1985) has made the interesting observation that even at quasi-static speeds (regime *a*) the deflection lagged the source by a distance of about 1 m. This is at variance with our theory, and Takizawa suggests it is a viscoelastic effect. Indeed Kenney (1954) has analysed the effect a load moving across an elastic plate supported by a Winkler base, with a damping force proportional to the vertical plate velocity. He found that damping caused the point of maximum depression to lag behind the load, and although the mechanics of this model is quite different from viscoelastic ice floating on water, it seems plausible to expect similar behaviour. At higher source speeds the lag increases but still remains larger than our theory predicts – e.g. when $V = c_{min}$ the observed lag is 3–4 m, whereas one-eighth of a wavelength is $\pi/4k_M = 2.3$ m. Equation (3.6) shows that for $V > c_{min}$ the lag increases to one quarter of a wavelength (see figures 4*e*, *f*), if term $R(X)$ is ignored. (This term must be retained to achieve a smooth transition in the lag as V increases through c_{min}.)

6. Conclusions

We have developed a theory to describe the wave system generated by an impulsively applied steadily moving line load. Asymptotic expansions as $t \to \infty$ give relatively simple formulae for the ice displacement, which show how the ice response changes with increasing source speed. Generally the displacement will tend to a steady form (relative to the source) modulated by transients which decay as $t^{-\frac{1}{2}}$ or sometimes $t^{-\frac{1}{3}}$, but at two critical speeds $V = c_{min}$ and $V = (gH)^{\frac{1}{2}}$ the displacement grows continuously because energy is not radiated away. The first of the critical speeds has long been recognised, but the second does not seem to have been described theoretically or experimentally, although Davys *et al.* (1985) recognise a transition in the wave pattern at this speed. Both represent a danger to vehicles on ice because of the continuous growth in ice deflections. Asymptotic analysis can also estimate the rate at which the disturbance propagates away from the source. When a steady wave pattern is generated it propagates away with the relative group speed, but at the critical speeds the propagation speed decays as $t^{-\frac{1}{4}}$ or $t^{-\frac{2}{5}}$.

The theory can be used to explain various anomalies in experimental observations. For example, displacement or stress amplification at $V = c_{min}$ is shown to be limited by the time that the source has been moving, as well as by viscoelasticity. Our estimates of stress amplification factors are about twice the reported experimental values – possibly because of their extreme sensitivity to vehicle speed. Discrepancies

between theoretical and observed gravity wavelengths are shown to arise because not enough time has elapsed for one complete wavelength to be propagated. One observation that this theory cannot explain however is the larger than expected lag of the point of maximum depression behind the source. As suggested by Takizawa (1985), it seems likely that this is a viscoelastic effect.

We are grateful to Professor R. J. Hosking for many enlightening discussions and helpful comments.

Appendix

We shall derive an asymptotic form as $t \to \infty$ for the integral

$$L(t) = -\int_{C_\epsilon} f(z) \frac{e^{iz^n t}}{z^2} dz \quad (n \geqslant 2),$$

where the function $f(z)$ is analytic in some neighbourhood of the origin and C_ϵ is the contour shown in figure 9. The contours C_ϵ for the two cases of particular interest – $n = 2$ and 3 – are also illustrated.

The function $f_2(z)$, defined by setting

$$f_2(z) = \frac{f(z)}{z^2} - \frac{f(0)}{z^2} - \frac{f'(0)}{z},$$

will be analytic in some neighbourhood of the origin, and we write

$$\begin{aligned} L(t) &= -f(0) \int_{C_\epsilon} \frac{e^{iz^n t}}{z^2} dz - f'(0) \int_{C_\epsilon} \frac{e^{iz^n t}}{z} dz - \int_{C_\epsilon} f_2(z)\, e^{iz^n t} dz, \\ &= -f(0)\, L_0(t) - f'(0)\, L_1(t) - L_2(t), \end{aligned} \tag{A 1}$$

say. Integrating by parts gives

$$\begin{aligned} \int_{C_\epsilon} \frac{e^{iz^n t}}{z^2} dz &= \text{change along } C_\epsilon \text{ of } \left(\frac{-1}{z} e^{iz^n t}\right) + int \int_{C_\epsilon} z^{n-2} e^{iz^n t} dz \\ &= int \int_{AO+OB} z^{n-2} e^{iz^n t} dz \end{aligned}$$

since the integrand is now analytic and the contour may be deformed. Making the substitutions

$$z = s e^{i\alpha} \quad \text{on } AO, \tag{A 2a}$$

$$z = s e^{i\beta} \quad \text{on } OB \tag{A 2b}$$

we find

$$-L_0(t) = (e^{-i\alpha} - e^{-i\beta})\, nt \int_0^\infty s^{n-2} e^{-s^n t} ds = (e^{-i\alpha} - e^{-i\beta})\, t^{1/n} \Gamma\left(\frac{n-1}{n}\right). \tag{A 3}$$

To evaluate $L_1(t)$ we note that

$$\int_{C_\epsilon} \frac{dz}{z} = \frac{-2\pi i}{n},$$

so we can re-express

$$-L_1(t) = \frac{2\pi i}{n} + \int_{C_\epsilon} \frac{1 - e^{iz^n t}}{z} dz. \tag{A 4}$$

Deforming the contour to the straight-lines segments AO, OB, and making the

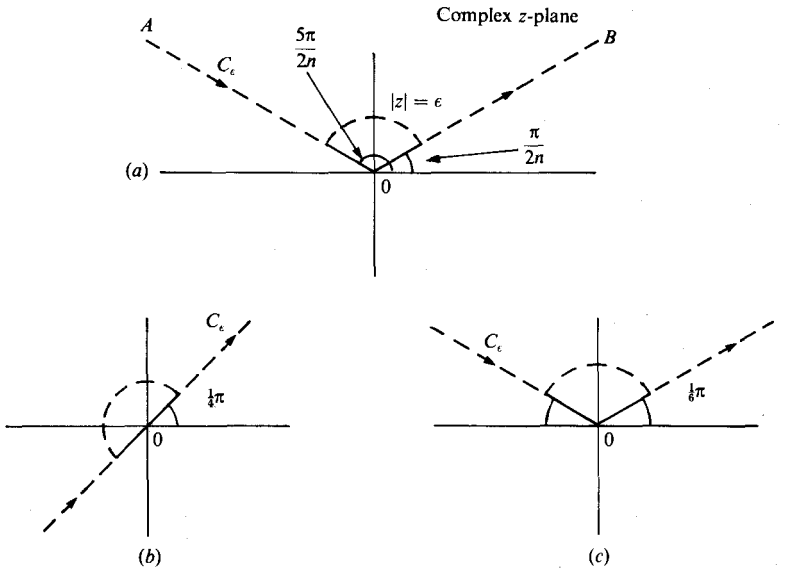

FIGURE 9. Diagram showing the integration contour C_ϵ, (*a*) for general n, (*b*) $n = 2$ and (*c*) $n = 3$.

substitutions (A 2*a*, *b*) as before, we find that the contributions of each segment to the integral in (A 4) cancel, so that

$$-L_1(t) = \frac{2\pi i}{n}. \tag{A 5}$$

Finally, suppose that $f_2(z)$ is analytic inside the circle $|k| = a$, and that $C_{\epsilon a}$ is the part of C_ϵ lying inside this circle. On the remaining part of C_ϵ the integrand in $L_2(t)$ is of order $e^{-a^n t}$, so

$$L_2(t) = \int_{C_{\epsilon a}} f_2(z)\, e^{iz^n t}\, dz + O(e^{-a^n t}). \tag{A 6}$$

It is easily shown by deforming the contour $C_{\epsilon a}$ to two finite straight-line segments and making the substitutions (A 2*a*, *b*) that the integral in (A 6) is of order $t^{-1/n}$, so combining (A 1), (A 3) and (A 5) we obtain

$$L(t) = f(0)\, t^{1/n} \Gamma\left(\frac{n-1}{n}\right)(e^{-\alpha i} - e^{-\beta i}) + f'(0)\frac{2\pi i}{n} + O(t^{-1/n}). \tag{A 7}$$

In the two particular cases of interest, $n = 2$ and 3, the asymptotic expansion (A 7) takes the form

$$L(t) = 2f(0)\, e^{-i\pi/4}(\pi t)^{\frac{1}{2}} + \pi i f'(0) + O(t^{-\frac{1}{2}}), \tag{A 8}$$

$$L(t) = f(0)\, t^{\frac{1}{3}} \sqrt{3}\, \Gamma(\tfrac{2}{3}) + \tfrac{2}{3}\pi i f'(0) + O(t^{-\frac{1}{3}}). \tag{A 9}$$

REFERENCES

BATES, H. F. & SHAPIRO, L. H. 1981 Stress amplification under a moving load on floating ice. *J. Geophys. Res.* **86**, 6638.

BELTAOS, S. 1980 Field studies on the response of floating ice sheets to moving loads. *Can. J. Civ. Engng* **8**, 1.

DAVYS, J. W., HOSKING, R. J. & SNEYD, A. D. 1985 Waves due to a steadily moving source on a floating ice plate. *J. Fluid Mech.* **158**, 269.

EYRE, D. 1977 The flexural motions of a floating ice sheet induced by moving vehicles. *J. Glaciol.* **19**, 555.

GREENHILL, A. G. 1887 Wave motion in hydrodynamics. *Am. J. Maths* **9**, 62.

KENNEY, J. T. 1954 Steady-state vibrations of beams on elastic foundations for moving loads. *Trans. ASME* E: *J. Appl. Mech.* **21**, 359.

KERR, A. D. 1981 Continuously supported beams and plates subjected to moving loads – a survey. *Solid Mech. Arch.* **6**, 401.

KERR, A. D. 1983 The critical velocities of a load moving on a floating ice plate that is subjected to inplane forces. *Cold Regions Sci. Tech.* **6**, 267.

KHEISIN, D. YE. 1963 Moving load on an elastic plate which floats on the surface of an ideal fluid (in Russian). *Izv. AN SSSR, OTN, Mekh. i Mashinostroenie*, 178.

KHEISIN, D. YE. 1971 Some non-stationary problems of dynamics of the ice cover. In *Studies in Ice Physics and Ice Engineering* (ed Iakolev). Israel Program for Scientific Translations.

LIGHTHILL, M. J. 1978 *Waves in Fluids.* Cambridge University Press.

NEVEL, D. E. 1970 Moving loads on a floating ice sheet. *US Army CRREL Res. Rep.* 261.

SCHULKES, R. M. S. M. 1986 Waves in floating ice plates due to a steadily-moving load. M.Sc. thesis, University of Waikato.

SQUIRE, V. A., LANGHORNE, P. J., ROBINSON, W. H. & HEINE, A. J. 1986 KIWI 131. An Antarctic field experiment to study strains and acoustic emission generated by loads moving over sea ice. Report prepared for the Royal Society of London.

SQUIRE, V. A., ROBINSON, W. H., HASKELL, T. G. & MOORE, S. C. 1985 Dynamic strain response of lake and sea ice to moving loads. *Cold Regions Sci. Tech.* **11**, 123.

TAKIZAWA, T. 1985 Deflection of a floating sea ice sheet induced by a moving load. *Cold Regions Sci. Tech.* **11**, 171.

WILSON, J. T. 1958 Moving loads on floating ice sheets. *University of Michigan Research Rep. UMRI Project* 2432.